(2004).

34. **Kim, M.-H., Kino-oka, M., Kawase, M., Yagi, K., and Taya, M.:** Response of human epithelial cells to culture surfaces with varied roughnesses prepared by immobilizing dendrimers with/without D-glucose display. J. Biosci. Bioeng., **103**, 111–119 (2007).

35. **Cox, E. A., Sastry, S. K., and Huttenlocher, A.:** Integrin-mediated adhesion regulates cell polarity and membrane protrusion through the Rho family of GTPases. Mol. Biol. Cell, **12**, 265–277 (2001).

Figure captions

FIG. 1. Time profiles of cellular morphology and roundness of typically selected epithelial cells cultured on various D-glucose-displayed surfaces. (A) 0% D-glucose display; (B) 50% D-glucose display; and (C) 100% D-glucose display. At 24 h of culture time, as indicated by the arrows, insulin (10 $\mu g/cm^3$) was added to the medium in the flasks.

FIG. 2. Efficiency of attachment and overall roundness of epithelial cells cultured on various D-glucose-displayed surfaces in the presence and absence of insulin. The error bars refer to standard deviation, SD (n = 3). Symbols: open circles; insulin-free medium, insulin (-); and closed circles; insulin-containing medium, insulin (+).

FIG. 3. Effects of GLUT and integrin blockings on efficiency of attachment of epithelial cells cultured on various D-glucose-displayed surfaces. The cells cultured for 24 h were subjected to the tests. The error bars refer to SD (n = 3). Symbols: closed circles, non-blocking; closed triangles, GLUT1-blocking; closed squares, GLUT4-blocking; closed diamonds, GLUT1 and 4-blocking; and closed reverted triangles, integrin $\alpha_5\beta_1$-blocking.

FIG. 4. Effects of GLUT blockings on overall roundness of epithelial cells cultured on various D-glucose-displayed surfaces. The cells cultured for 24 h were subjected to the tests. The error bars refer to SD (n = 3). Symbols: closed circles, non-blocking; closed triangles, GLUT1-blocking; closed

squares, GLUT4-blocking; and closed diamonds, GLUT1 and 4-blocking.

FIG. 5. Immunostaining of actin cytoskeleton (green) and vinculin (red) of epithelial cells cultured on various D-glucose-displayed surfaces in the presence of insulin (A, B) and absence of insulin (C, D, E). The images show the representative cells cultivated on the surfaces with 0% (A, C), 50% (D) and 100% D-glucose (B, E) display.

FIG. 6. Immunostaining of actin cytoskeleton (green), and GLUTs1 and 4 (red) of cells cultured on various D-glucose-displayed surfaces in the presence of insulin (A, B) and absence of insulin (C, D). The images show the top and side (cross-section) views of the representative cells cultured on the surfaces with 0% (A, C) and 100% D-glucose (B, D) display. The white and yellow arrows represent the apical and basal sides of cells, respectively, the latter side being in contact with the culture surface.

FIG. 7. Schematic illustration showing possible mechanism of morphological change of epithelial cells in relation to GLUT-mediated anchoring onto D-glucose-displayed surface.

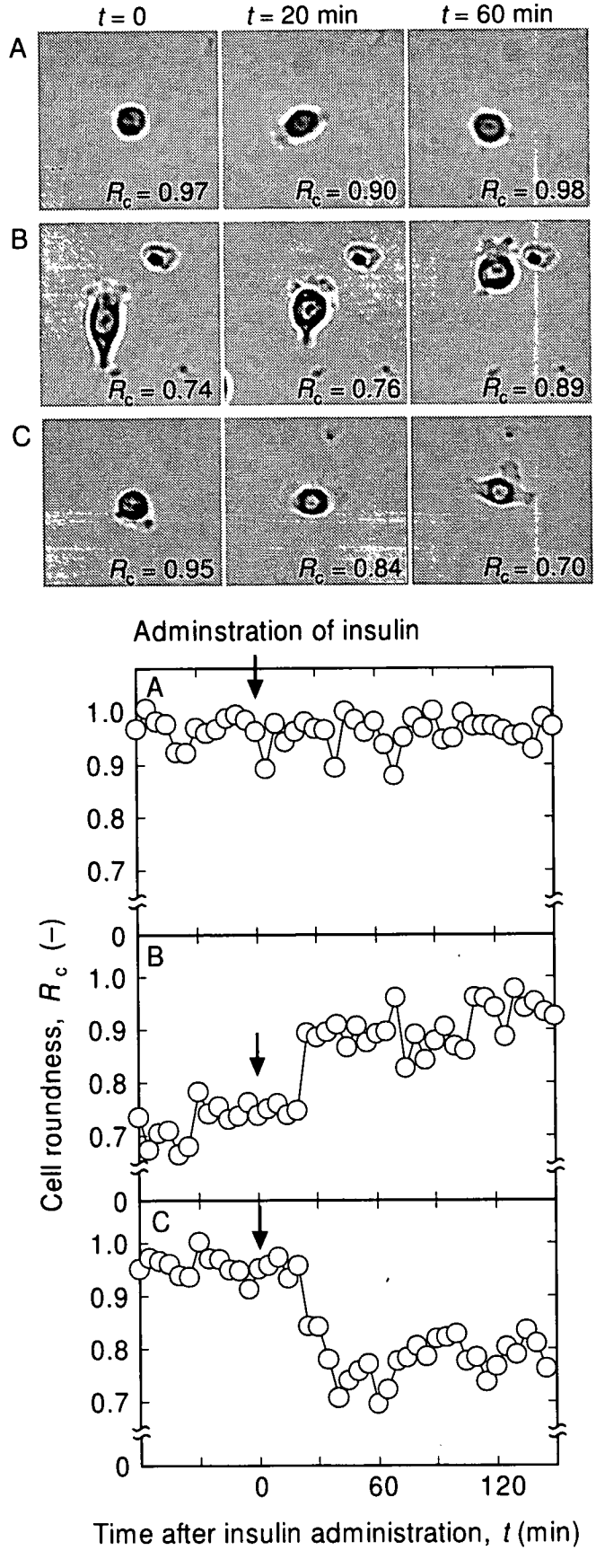

FIG. 1, Kim et al.

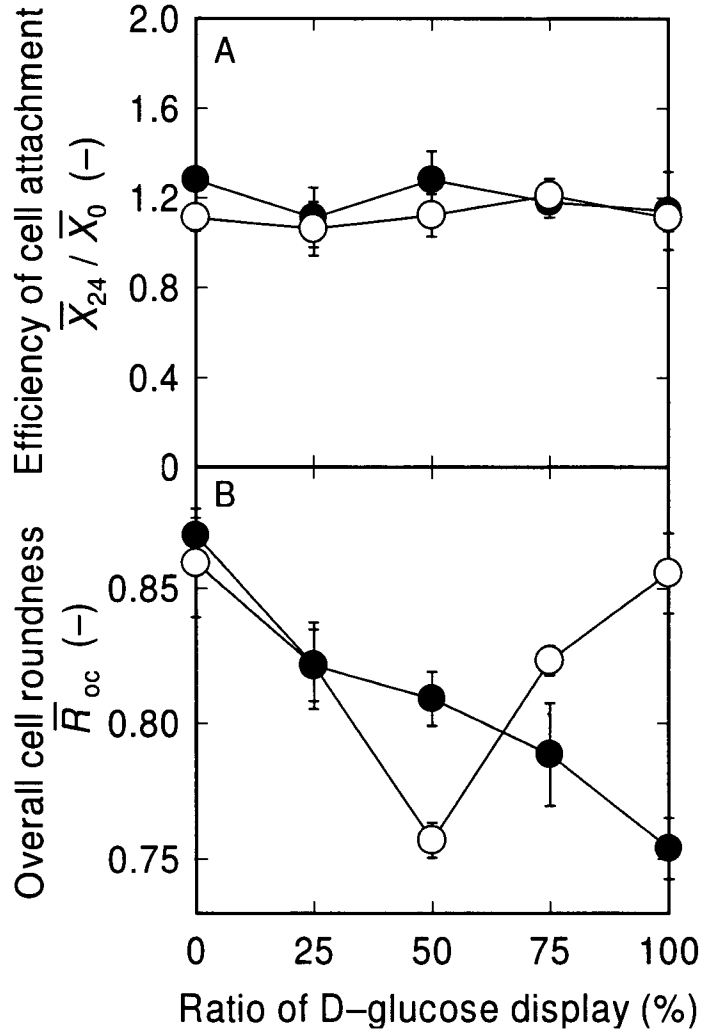

FIG. 2, Kim et al.

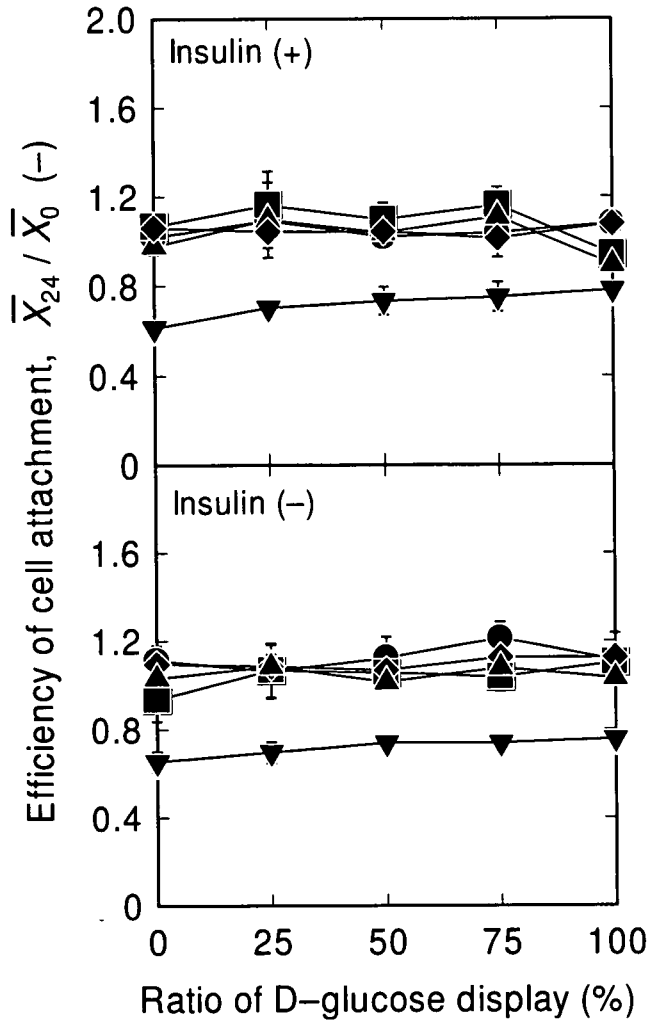

FIG. 3, Kim et al.

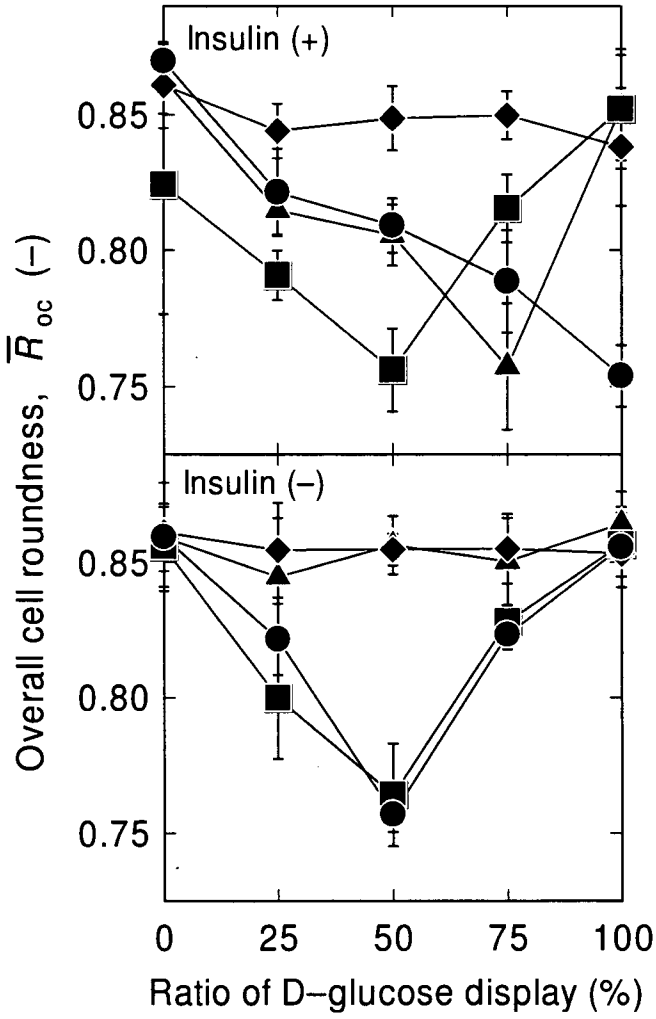

FIG. 4, Kim et al.

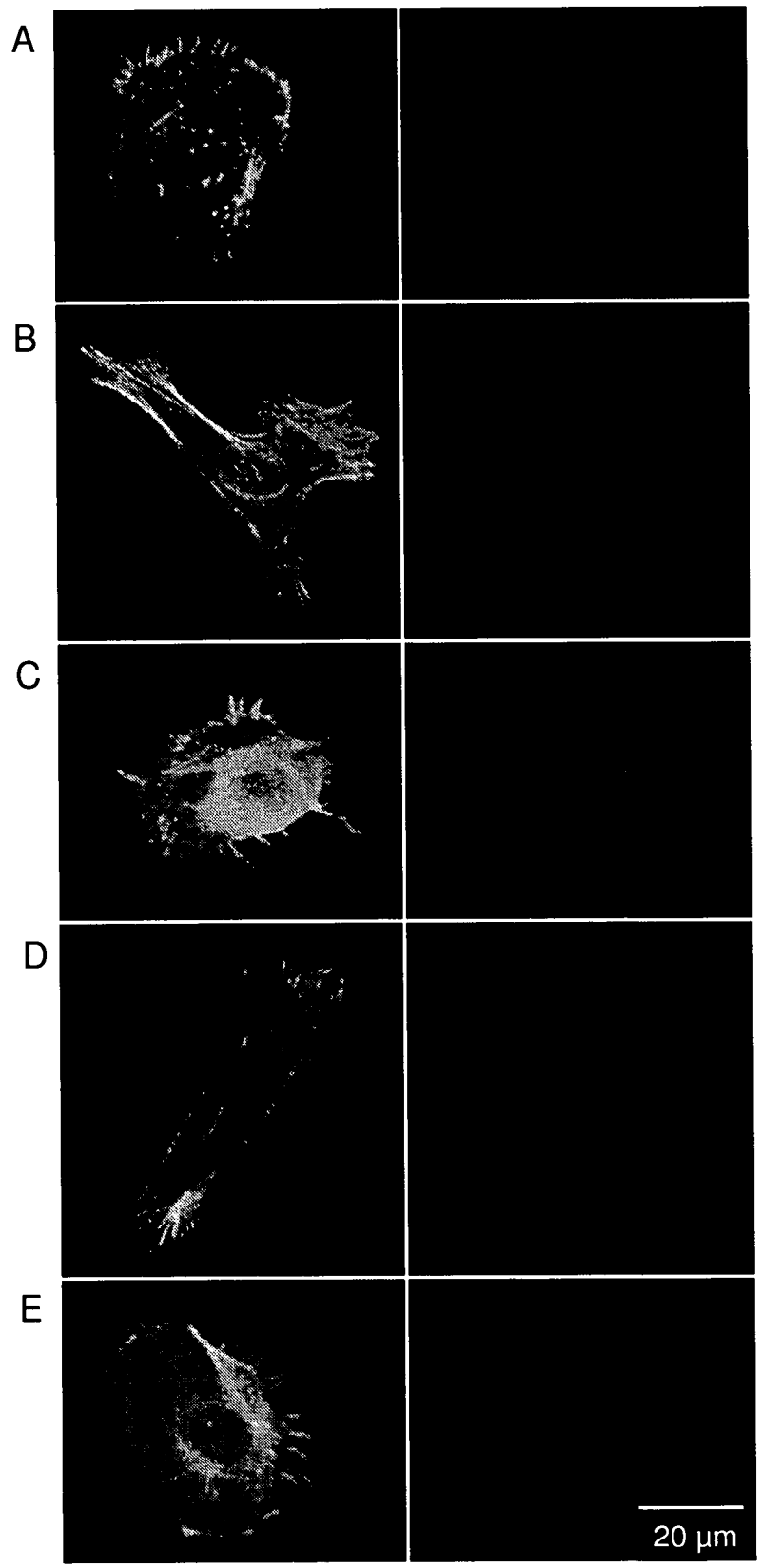

FIG. 5, Kim et al.

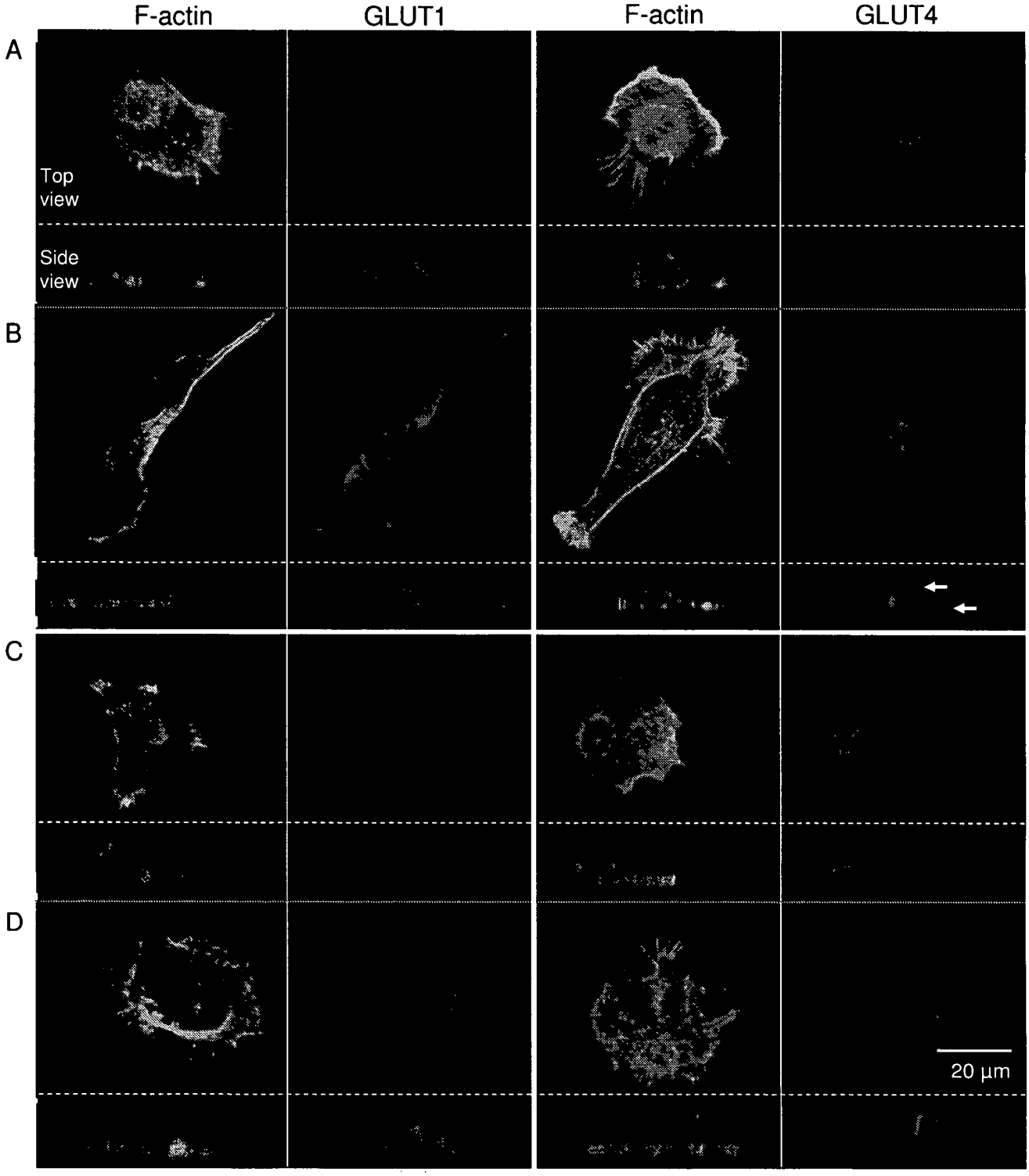

FIG. 6, Kim et al.

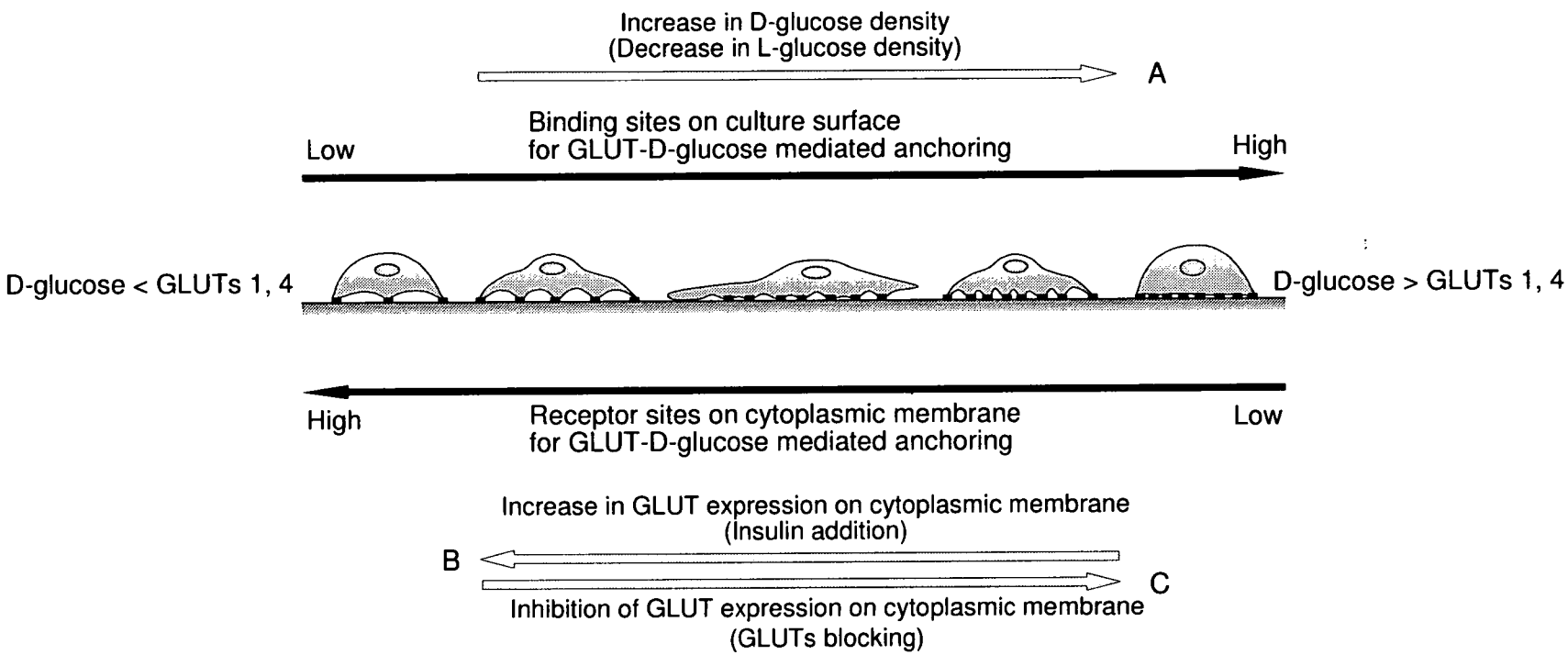

FIG. 7, Kim et al.

JOURNAL OF BIOSCIENCE AND BIOENGINEERING
Vol. 103, No. 2, 192–199. 2007
DOI: 10.1263/jbb.103.192

Response of Human Epithelial Cells to Culture Surfaces with Varied Roughnesses Prepared by Immobilizing Dendrimers with/without D-Glucose Display

Mee-Hae Kim,[1] Masahiro Kino-oka,[2] Masaya Kawase,[3] Kiyohito Yagi,[4] and Masahito Taya[1,2]*

Department of Biotechnology, Graduate School of Engineering, Osaka University, 2-1 Yamada-oka, Suita, Osaka 565-0871, Japan,[1] Division of Chemical Engineering, Graduate School of Engineering Science, Osaka University, 1-3 Machikaneyama-cho, Toyonaka, Osaka 560-8531, Japan,[2] Faculty of Pharmaceutical Sciences, Osaka Ohtani University, 3-11-1 Nishiki-ori, Tondabayashi, Osaka 584-8540, Japan,[3] and Graduate School of Pharmaceutical Sciences, Osaka University, 1-6 Yamada-oka, Suita, Osaka 565-0871, Japan[4]

Received 26 September 2006/Accepted 1 December 2006

To investigate the response of human epithelial cells to substrates with nanoscale modifications, dendrimer-immobilized surfaces were prepared with or without D-glucose displayed as a terminal ligand, giving topographic structures with mean roughnesses (R_a) of 1.8–11.0 nm. With an increase in the R_a value up to 4.0 nm, the epithelial cells cultured on naked dendrimer surface without D-glucose display were somewhat stretched in their morphology compared with those on a nonmodified plain surface. However, for the R_a values higher than 4.0 nm, such cell stretching was inhibited, resulting in the predominant existence of round-shaped cells. The change in cell morphology was appreciable on the surfaces with D-glucose-displayed dendrimers. When the R_a value increased up to 4.5 nm on these surfaces, in particular, the enhancement of cell stretching was recognized, and fluorescence microscopic observation supported the hypothesis that the glucose-transporter-mediated adhesion of cells to the surface encouraged the development of filopodia and stress fibers, thereby improving focal contact with the surface. Our results suggest that the combination of displaying D-glucose and modulating roughness can promote cytoskeletal formation accompanied by marked cell elongation on culture surfaces.

[**Key words:** human epithelial cells, dendrimer-immobilized surface, glucose display, nano-scale roughness, cell roundness, cytoskeleton, glucose transporter]

The adhesion of anchorage-dependent cells to underlying substrates modulates a variety of cellular events such as signaling, gene expression and proteogenic changes. This process involves interactions of extracellular matrix (ECM), *e.g.*, fibronectin, with the integrin family of transmembrane receptors. Integrins are major transmembrane ECM receptors and function as bidirectional transducers of signals and mechanical forces (1, 2). The integrin-mediated interactions of cells with ECM involve the formation of focal adhesion sites, which regulate signaling processes. These structurally defined adhesion sites are associated with cytoskeletal proteins by complicated mechanisms. The series of events involves the development of focal contact along with the recruitment of various cytoskeletal proteins (3, 4). The reciprocal cross-talk between these cytoskeletal systems and their adjoining substrates can give clues that can help unravel the critical regulatory pathways relating to cell morphology and motility (5, 6). Recent reports have provided new insights into these physiological interactions with respect to the process of cell adhesion to topographic surfaces (7–10). For example, it was demonstrated that the surface topography of substrates affects the cellular extension accompanied by filopodium development, indicating the existence of a favorable surface roughness on the nanoscale (11–13).

According to a review by Dalby *et al.* (13), cells encounter different topographies, ranging from macro- (tissue level) to micro- (cell level) or to nano-scales (organelle and protein levels). Microscale topographies induce changes in cell adhesion, morphology, motility and gene expression. It is most likely that these surfaces have the potential to regulate tissue organization and cell differentiation (14). On the other hand, cells are generally surrounded by nanoscale structural cues that may also be involved in controlling cell responses. Recently, manufacturing techniques for nanoscale fabrication, such as electron-beam or colloidal lithography and polymer demixing, have been made available for cell manipulations (15). Surface topography induces cellular responses to the physical architectures of substrates by affecting cell morphology, migration, proliferation and differenti-

* Corresponding author. e-mail: taya@cheng.es.osaka-u.ac.jp
phone: +81-(0)6-6850-6251 fax: +81-(0)6-6850-6254

ation (9–17).

Dendrimers are attractive owing to their chemical characteristics, because it is quite easy to modify their chemical properties by adjusting their terminal groups (18, 19). Starburst polyamidoamine (PAMAM) dendrimers are highly branched spherical polymers with well-defined structures that are soluble in aqueous solutions and have a unique surface composed of primary amino groups. PAMAM dendrimers have a core molecule, either an ammono residue as a trivalent initiator core or an ethylenediamine residue as a tetravalent initiator core, which is used to prime the stepwise polymerization, that determines several structural characteristics such as bulk, shape, density, and electrostatic charge. When an additional layer or generation is polymerized on dendrimer molecules, the number of terminal amino groups is doubled. Therefore, the defined structure and large number of terminal amino groups on dendrimers make these polymers suitable for use as biocompatible nanocapsules in gene or drug delivery systems, because of their flexibility in design variables including the ligand species present on the terminal groups as well as dendrimer size and ligand density (19–21).

In our previous studies, the potential of using dendrimers for cell processing was extended by applying this compound to a culture substratum for cell growth and differentiation. The immobilization of dendrimer was carried out to prepare the scaffold for rat hepatoma cells, and modifications of amino groups with various ligands were carried out for enhancing viability and hepatopoetic functions (22–24). In addition, a dendrimer substrate displaying D-glucose exerted a strong effect on the cellular morphology of human keratinocytes (25). In this study, various dendrimer-immobilized surfaces were prepared with different architectures by changing the generation number of dendrimers and they were characterized in terms of surface roughness by atomic force microscope (AFM). Moreover, the cellular response of human epithelial cells cultured on these surfaces was examined in terms of morphological behaviors.

MATERIALS AND METHODS

Surface modification The conventional plastic culture surface of a square 8-well plate (surface area, 8.6 cm^2; Nunc, Roskilde, Denmark) was used as a plain or starter material. Surfaces with different topographies were obtained by immobilizing dendrimers, which were prepared through the accumulation or spherical method as illustrated in Fig. 1.

The dendrimer surfaces were designed as follows on the basis of

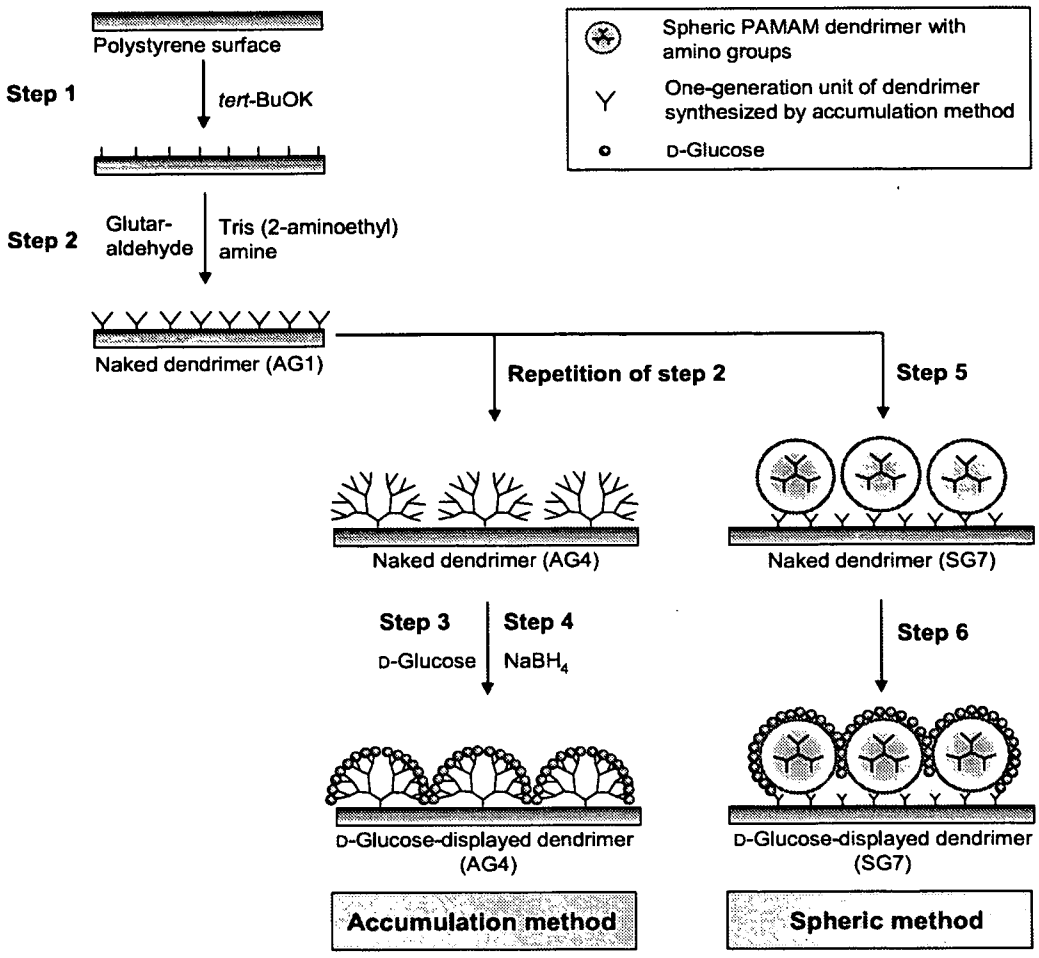

FIG. 1. Schematic illustration of processes to obtain dendrimer-immobilized surfaces with/without D-glucose display. AG and SG denote dendrimers synthesized by the accumulation and spheric methods, respectively, with the numericals showing the generation number of dendrimers.

the accumulation method. A first-generation dendrimer (denoted as AG1) was immobilized by the four-step reaction conducted under a sterile condition. Step 1: To display a hydroxyl group on the plain surface, a solution containing 50 μmol/ml potassium *tert*-butoxide (*tert*-BuOK) was poured into each well, and then the wells were incubated for 1 h at ambient temperature. The wells were then washed three times with sterilized water. The dendron core density depended on the quantity of hydroxyl groups displayed at the onset of synthesis, which can be regulated by adjusting the concentration of *tert*-BuOK. Step 2: An aqueous solution of 360 μmol/ml glutaraldehyde was introduced into the wells. The wells were allowed to stand for 1 h, followed by washing with a large amount of sterile water. The wells were then treated with 360 μmol/ml tris(2-aminoethyl) amine solution (pH 9.0, adjusted with 1 mol/dm^3 NaOH) for 1 h to produce a dendron structure and then rinsed with sterile water. Step 3: To display D-glucose as a terminal ligand, $0.1\times2^{n-1}$ μmol/ml D-glucose solution was added to and left to sit in the wells for 2 h (n: generation number). Step 4: A sodium borohydride solution (0.5 μmol/ml) was poured into the wells, and after being left to stand for 24 h, the wells were washed with sterile water, yielding the surface of first-generation dendrimer with D-glucose display. For the preparation of a culture surface with naked dendrimers (only amino group displayed), step 3 was omitted from the above-mentioned procedures.

High-generation dendrimers were prepared as follows. A solution of 360 μmol/ml glutaraldehyde was added to each well after step 2. After washing the well as described above, step 2 was conducted again. These operations were repeated until the desired generation number of dendrimers was reached. Thereafter, steps 3 and 4 were carried out for the modification of the dendrimers with D-glucose as a ligand.

The spheric method was used to prepare dendrimer surfaces with a relatively high degree of roughness. Substrates modified with spheric dendrimers at their terminal amino group were produced on the well as follows. On the first-generation dendrimer surface prepared through steps 1 and 2 by the accumulation method, spheric dendrimers were immobilized by the following reactions. Step 5: To crosslink the amino groups of spheric dendrimers, an aqueous solution of 360 μmol/ml glutaraldehyde was poured into the wells. The wells were allowed to stand for 1 h, followed by washing with a large amount of sterile water, and then a 0.05 % (v/v) aqueous solution of PAMAN spheric dendrimer (Sigma-Aldrich, St. Louis, MO, USA) was placed on the surface and left to stand for 3 h. The spheric dendrimer-immobilized surface was then rinsed with sterilized water to remove the unbound dendrimer molecules. Step 6: D-Glucose was displayed on the terminal group of immobilized dendrimers by carrying out steps 3 and 4. When necessary, the repeated steps for increasing the generation number of immobilized dendrimers, as described above, were added before step 6.

Cell culture A line of human mammary epithelial cells (hTERT-HME1; Clontec Laboratories, San Diego, CA, USA), which were genetically modified to have an extended cell span, was obtained as frozen cells. The cells, which were in vials, were thawed according to the supplier's manual, and then incubated in a 25-cm^2 T-flask (Nunclon Delta Flask; Nunc, Roskilde, Denmark). Unless otherwise stated, the cells were cultivated in serum-free medium containing 10 μg/ml insulin (HuMedia-KG2; Kurabo Industries, Osaka) at 37°C under a 5% CO_2 atmosphere as described elsewhere (25). For the experiments, the seeding density of viable cells, determined by trypan blue exclusion, was set at $X_0=3.0\times10^3$ cells/cm^2.

To estimate the concentration of adherent cells, the bottom surface image of each well was captured from three different positions using a CCD camera (CS6931; Toshiba Teli, Tokyo) attached to a microscope (area of captured image: 2.4 mm^2). The projected area, A_c, and the periphery length, l_c, of each cell in the cultures were determined by extracting the cellular edge on the images using a line-drawing tool on a software package (IMAQ Vision; National Instruments, Austin, TX, USA). The degree of roundness, R_c, of each cell was defined as follows.

$$R_c=\frac{2(\pi A_c)^{1/2}}{l_c};\ 0<R_c\leq1 \quad (1)$$

The mean value of R_c was recorded as the mean of data from 50–120 cells.

Confocal laser-scanning microscopy The cells were subjected to F-actin and vinculin stainings as follows. The cells were fixed for 10 min at room temperature with 4% paraformaldehyde in phosphate-buffered saline (PBS), followed by being soaked in PBS with 0.1 % Triton X-100 for 4 min. The cells were then kept at 4°C for 24 h with a primary antibody against vinculin (1:400, Sigma-Aldrich) after masking nonspecific proteins for 1 h at room temperature using Block Ace (Dainippon Pharmaceutical, Osaka). The cells were washed with Tris-buffed saline (DakoCytomation Carpinteria, CA, USA), followed by immunolabeling with Alexa Fluor 594 goat anti-mouse IgG (Molecular Probes, Eugene, OR, USA) for vinculin and Alexa Fluor 488 phalloidin (Molecular Probes) for F-actin. The samples were observed under a confocal laser scanning microscope (model FV-300; Olympus, Tokyo).

Atomic force microscopy (AFM) An atomic force microscope (NanoScope IIIa, Digital Instruments, Santa Barbara, CA, USA) was used to characterize the topography of the prepared culture surfaces. Sample was attached to an AFM specimen disk. All the samples were analyzed in a dry state and examined in Tapping Mode with standard silicon tips (NCH-10V; Digital Instruments). The scan size of each surface was 1×1 μm at a rate of 1 Hz on 256 scanning lines. The analysis of topography including surface denomination was carried out using the commercially available software (SurftopEye, Mitani, Fukui). Mean roughness, R_a, was determined from the measurements in triplicate regions of independently prepared surfaces.

RESULTS

Surface design and topography Five types of naked dendrimer surfaces, which bore an amino group as a terminal ligand, were designed by changing the generation number of dendrimers according to the preparation methods shown in Table 1. The topography of the surface was evaluated using the defined parameter of mean roughness, R_a. The plain surface of the well was characterized to be $R_a=0.2$ nm. With an increase in the generation number of dendrimers

TABLE 1. Mean roughnesses of prepared surfaces with dendrimers (no D-glucose display)

Surface		R_a (nm)
Plain surface		0.2±0.0
Prepared by accumulation method	AG1	1.8±0.2
	AG2	2.5±0.0
	AG3	3.5±0.6
	AG4	4.0±0.3
	AG5	3.6±0.1
	AG6	4.0±0.9
Prepared by spheric method	SG7	6.8±0.4
	SG7 AG3[a]	7.9±0.7
	SG7AG5[a]	11.0±0.6

[a] The spheric dendrimer was first immobilized on the surface (SG7) according to the procedure shown in Fig. 1, and then the accumulation method was applied for a further increase in the generation number of dendrimers.

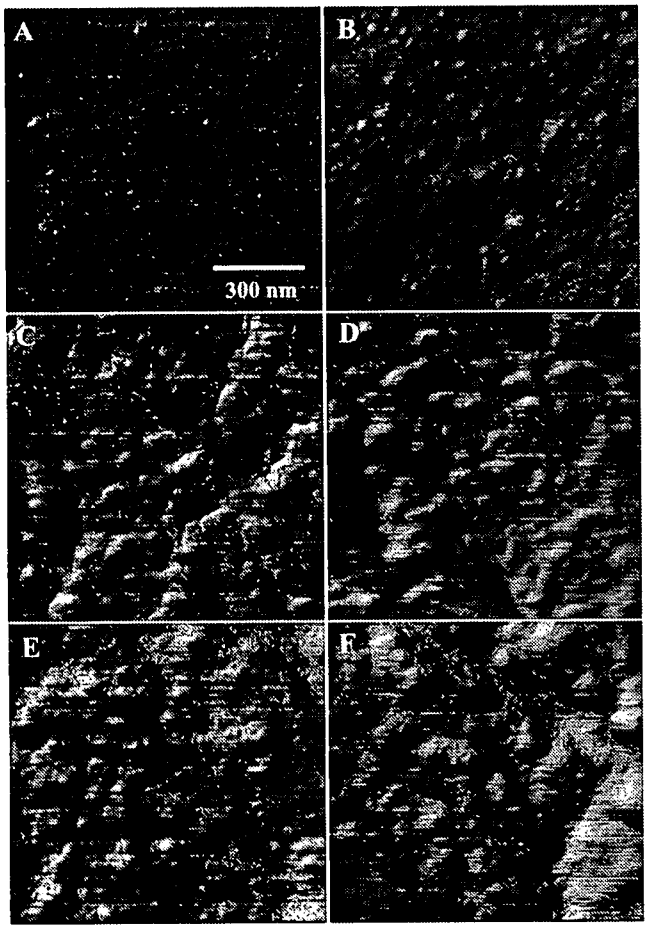

FIG. 2. Representative AFM images of naked dendrimer surfaces. (A) Plain, (B) AG1, (C) AG4, (D) AG6, (E) SG7AG3 and (F) SG7AG5 surfaces.

for the accumulation method, the R_a value increased, giving R_a=4.0 nm for the 4th-generation dendrimer surface (denoted as AG4). On the contrary, the value of R_a did not increase for the naked dendrimer surface of the 5th or 6th generation (3.6 nm for AG5 and 4.9 nm for AG6).

The spherical dendrimer was thought to produce a higher degree of roughness on the surface owing to its structure. In this study, spherical dendrimers of the 7th generation, which possessed a theoretical diameter of 8.1 nm (19), were immobilized as a framework of the convex surface. The R_a value of this surface (denoted as SG7 in Table 1) reached 6.8 nm, and further development caused an increase in the R_a value, yielding R_a=11.0 nm for the SG7AG5 surface, which had the highest R_a value of the dendrimer surfaces prepared in this study. Figure 2 shows the architectures of the selected surfaces. According to the R_a value, indented topographies were observed on the respective dendrimer surfaces; in contrast, the plain surface exhibited a relative smoothness. For the D-glucose-displayed dendrimer surfaces prepared, similar topographies were recognized, and their R_a values were slightly higher than those of the naked dendrimer surfaces (data not shown). Thus, variation in the generation numbers and preparation methods can endow surfaces with different nanoscale topographies.

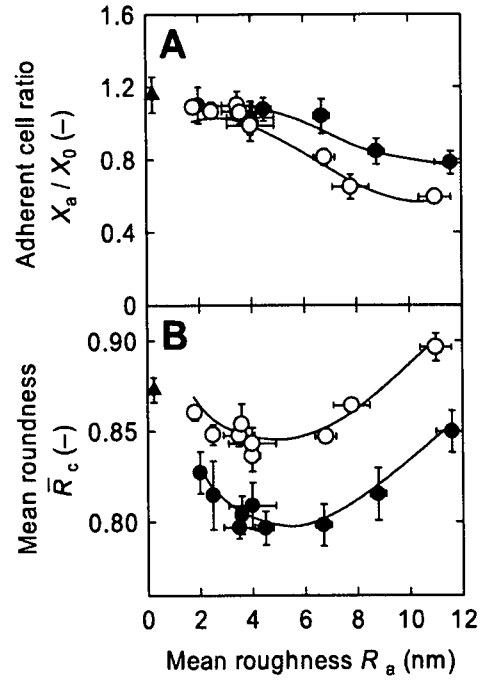

FIG. 3. Effects of mean roughness on attachment and morphology of human epithelial cells cultured on various dendrimer-immobilized surfaces. Plots of (A) X_a/X_0 and (B) $\bar{R}_c$ against R_a, determined at 24 h of culture time. Error bars indicate standard deviations (n=3). Symbols: closed circles, D-glucose-displayed dendrimer surface; open circles, naked dendrimer surface; and closed triangles, plain surface.

Attachment of cells to designed surfaces To investigate cellular responses to the naked and D-glucose-displayed dendrimer surfaces, the cultures of human epithelial cells were conducted, and 24 h after seeding, the ratio of adherent cells to seeded cells, X_a/X_0, was determined. As shown in Fig. 3A, with an increase in the R_a value of the naked dendrimer surface, the value of X_a/X_0 decreased (X_a/X_0=0.6 when R_a=11.0 nm), while the X_a/X_0 value on the plain surface was 1.2. The X_a/X_0 values of the D-glucose-displayed dendrimer surfaces also decreased with an increase in the R_a value, although the level of X_a/X_0 was slightly higher than that of the naked dendrimer surface with larger value of R_a. These results suggest that roughness can inhibit cellular access to the surface and that the display of D-glucose suppress such inhibition to some extent.

Cellular morphology on designed surfaces To investigate the interaction between the cells and surfaces, cellular morphology was observed 24 h after seeding. With an increase in the R_a value up to 4.0 nm, the cells on the naked dendrimer surface were somewhat stretched. The cellular morphology was quantified in terms of the mean degree of cell roundness, $\bar{R}_c$. As shown in Fig. 3B, on the naked dendrimer surfaces with the R_a values up to 4.0 nm, a slight decrease in $\bar{R}_c$ value was found compared with the $\bar{R}_c$ value of the plain surface. A further increase in the R_a value, however, caused less cell extension with an increase in $\bar{R}_c$ value, and round-shaped cells prevailed with $\bar{R}_c$=0.9 at R_a=11.0 nm. For D-glucose-displayed dendrimer surfaces, the morphological change with the R_a value showed a similar tendency to that of the naked dendrimer surface, although the increase

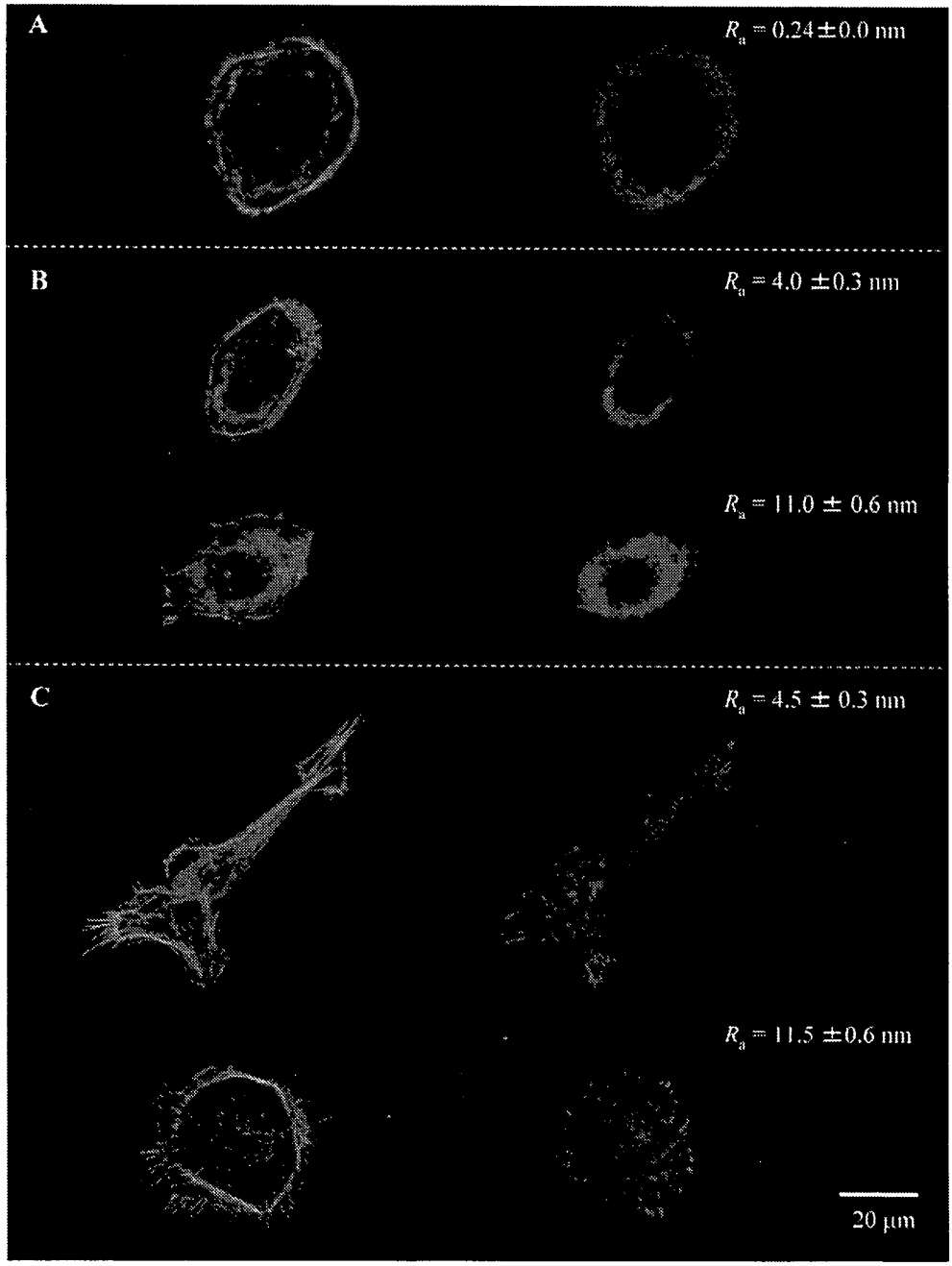

FIG. 4. Immunostaining of actin cytoskeleton (green) and vinculin (red) of human epithelial cells cultured for 24 h on dendrimer-immobilized surfaces with various values of mean roughness. (A) Plain, (B) naked dendrimer and (C) D-glucose-displayed dendrimer surfaces.

in the population of stretched-shape cells was significant, resulting in the lower values of $\bar{R}_c$ in the entire range of R_a values examined. On the D-glucose-displayed dendrimer surface at R_a=6.7 nm, the value of $\bar{R}_c$ was minimized to 0.8, which is much smaller than the minimal $\bar{R}_c$ value of the naked dendrimer surface at R_a=4.0 nm. Thus, the cell morphology was remarkably altered as a result of the roughness of the culture surface.

To clarify the cytoskeletal organization and focal contact with the dendrimer surface, the cells were observed 24 h after seeding by the fluorescence stainings of F-actin and vinculin. As seen in Fig. 4B, the epithelial cells cultured on the naked dendrimer surface with R_a=4.0 nm were abundant in F-actin filaments of peripheral stress fibers and filopodia, compared with those cultured on the plain surface (Fig. 4A). However, the cells on the naked dendrimer surface with R_a=11.0 nm showed a poor organization of stress fibers with punctuate actin as well as less developed filopodia (Fig. 4C). For the cells on the D-glucose-displayed dendrimer surfaces with R_a=4.5 nm, on the other hand, fully organized actin stress fibers with distinct vinculin spots appeared in both the cytoplasm and the cell periphery, whereas nebular vinculin was only observed in the cell periphery on the corresponding naked dendrimer surfaces (Fig. 4B). For the

cells on the D-glucose-displayed dendrimer surface with R_a=11.5 nm, the stress fibers in cytoplasm disappeared. Thus, the cell staining analyses revealed that surface roughness affects the formation of F-actin filaments which are used to organize filopodia and stress fibers. In addition, the D-glucose display enhanced the development of stress fibers with distinct spots of vinculin. These findings support the hypothesis that the grasping of the glucose transporter in the cytomembrane with D-glucose immobilized on the surface facilitates the frequent formation of cell-surface contact.

DISCUSSION

Culture surface is a kind of reaction field in which anchorage-dependent cells show behaviors of attachment, migration and division. Many researchers have paid their attention to gene transfer and the stimulation of receptors on the plasma membrane through interactions with solid surfaces. The interactive effectiveness of biologically active components can be improved by arraying them in close contact with targets on the cell membrane, because the dispersed components in bulk liquid (medium) are less able to approach the targets. The methodological development of component display on culture surfaces is considered to be one of the most critical issues. Dendrimers have recently become of interest as synthetic chemicals that provide a promising template for an effective gene delivery system obtained by changing the generation number of dendrimers and ligand species. When dendrimers are deposited on a solid surface, their unique properties are expected to yield physical and chemical variations in surface roughness, dendrimer density, and ligand species attached to and their amounts on the dendrimers, together with the locality of displayed ligands. In the present study we focused on the influences of roughness and ligand type on the cellular response by changing the generation number of dendrimers with or without D-glucose display.

Surface roughness governs cell morphology, which depends on cytoskeletal formation involving the development of actin stress fibers and dynamic links with filopodia. Dalby *et al.* (13) reported that the development of F-actin filaments is promoted in fibroblasts on a surface modified with a moderate roughness, even though excess roughness inhibited such development, being poor in attachment of round-shaped cells compared with that on a nonmodified plain surface. This trend was concordant with our results obtained in the cultures of epithelial cells on the dendrimer surfaces with various mean values of roughness. Filopodium development in the cells on the naked AG4 dendrimer surface (R_a=4.0 nm) was promoted compared with that in the cells on the plain surface. However, a further increase in degree of roughness suppressed its development, and the cells cultured on the naked SG7AG5 dendrimer surface (R_a=11.0 nm) exhibited punctuate and nebulous actins (see Fig. 4).

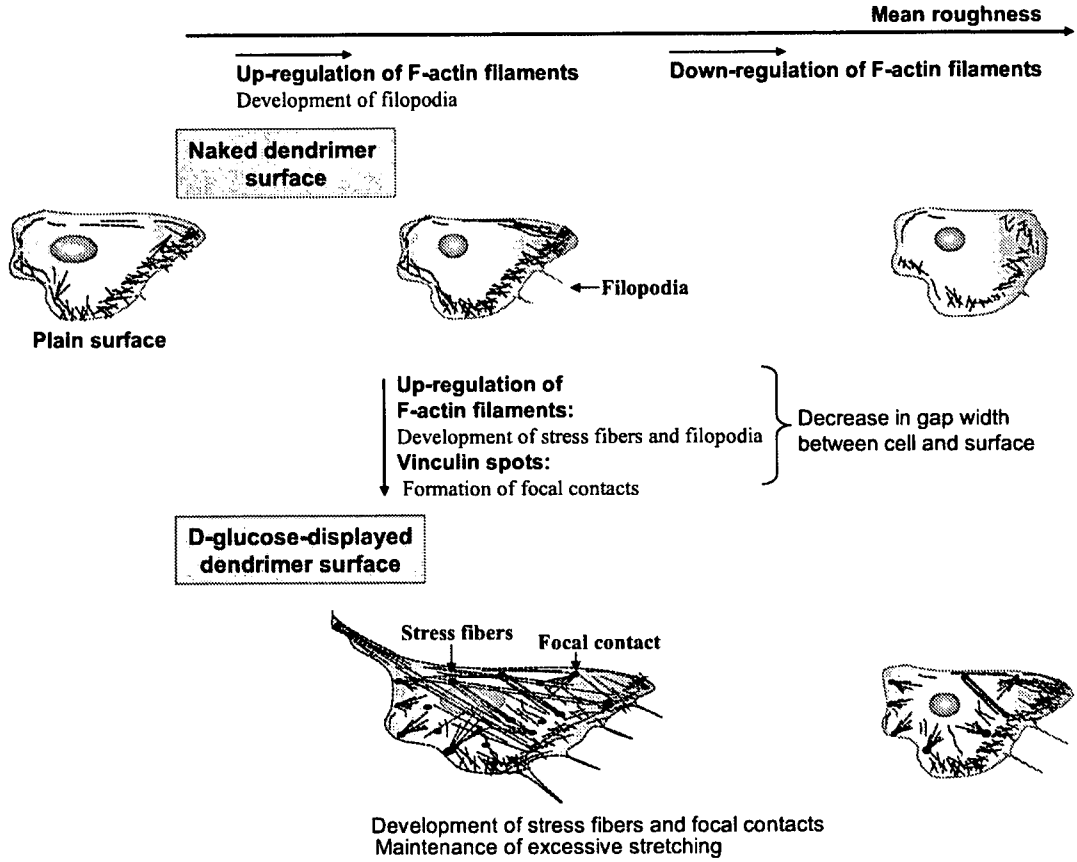

FIG. 5. Conceptual illustration showing morphological changes of human epithelial cells cultured on various dendrimer-immobilized surfaces with/without D-glucose display.

Surfaces with the functional groups of biologically active molecules have been designed for targeting integrins and their receptors on cellular membrane (26, 27). Current researches have been focused on developing surfaces modified with physicochemically well-defined, biomimetic materials that have various properties such as a low protein-adsorbing, for dealing with the control of cytomembrane-mediated interactions to promote cellular functions (28–30).

The uptake of D-glucose from medium is mediated through the glucose transporters (GLUTs), which essentially have no affinity for its optical isomer L-glucose on the plasma membrane of cells. Therefore, D-glucose display on surfaces enable its binding to ventral GLUTs on the membrane, which permits the cells to anchor partially by temporally grasping GLUTs. In addition, cell migration relates dynamically to the assembly of filopodium actin filaments appearing at the leading edge and the disassembly of such filaments at the tail, which are responsible for the extension and retraction of cells, respectively. The partial anchoring through GLUTs seems to prevent retraction in the rear of cells based on the consideration that the suppression of filament disassembly causes excessive cellular elongation. This idea supports the view that GLUTs may make a certain contribution to the cellular elongation observed in this study. With regard to dynamic links and cytoskeleton formation, D-glucose display on the surface induced clearly defined actin filaments of filopodia and stress fibers, respectively (see Fig. 4). In addition, the vinculin spots at the terminals of stress fibers indicated mature focal contacts, unlike for the naked dendrimer surface, on which the cells exhibited a smaller number of actin filaments with nebular vinculin expression. The changes in cell shape as well as the potentials of anchorage and motility are mainly associated with a dynamic reorganization of the filament arrays that make up the actin cytoskeleton. The activation of individual members of the Rho family (small G proteins) modulates the organization of actin filaments in cells, with Rho activation resulting in the formation of stress fibers with focal contacts, which are involved in the formations of Rac-inducing lamellipodia and Cdc42-inducing filopodia (4).

Figure 5 illustrate a possible mechanism of the morphological response of epithelial cells to the dendrimer-immobilized surfaces with or without D-glucose display. It is proposed that D-glucose displayed on dendrimers permits the cells to be in close contact with the surface through the grasping of GLUTs on the plasma membrane, being attributable to the up-regulation of focal contact formation. In addition, this GLUT-mediated grasping promoted the development of stress fibers in the cytoplasm particularly at moderate mean roughnesses of approximately 4.5 nm, resulting in the excessively stretched shape of cells. Therefore, surface roughness and D-glucose display induce changes in cellular morphology caused by alternation in the cytoskeleton in response to focal contact formation. In conclusion, in this study, we propose that dendrimer surfaces will offer a promising design for human epithelial cell stimulators by the surface-localized display of suitable ligands targeting receptors on cell membrane.

ACKNOWLEDGMENTS

This study was conducted as part of the programs "Center for integrated cell and tissue regulation" for the Center of Excellent (21st COE) and "Multidisciplinary research laboratory system" organized in the Graduate School of Engineering Science, Osaka University. This study also received financial support in part by a Grant-in-Aid for Scientific Research (no. 17360398) from the Ministry of Education, Culture, Sports, Science and Technology and by a grant for Research on Human Genome, Tissue Engineering and Food Biotechnology from the Ministry of Health, Labour, and Welfare, Japan.

REFERENCES

1. **Martin, K. H., Slack, J. K., Boerner, S. A., Martin, C. C., and Parsons, J. T.:** Integrin connections map: to infinity and beyond. Science, **296**, 1652–1653 (2002).
2. **Gumbiner, B. M.:** Cell adhesion: the molecular basis of tissue architecture and morphogenesis. Cell, **84**, 345–357 (1996).
3. **Geiger, B., Bershadsky, A., Pankov, R., and Yamada, K. M.:** Transmembrane crosstalk between the extracellular matrix-cytoskeleton crosstalk. Nat. Rev. Mol. Cell Biol., **2**, 793–805 (2001).
4. **Sastry, S. K. and Burridge, K.:** Focal adhesions: a nexus for intracellular signaling and cytoskeletal dynamics. Exp. Cell Res., **261**, 25–36 (2000).
5. **Bernhard, W. H. and Beat, A. I.:** Actin, microtubules and focal adhesion dynamics during cell migration. Int. J. Biochem. Cell Biol., **35**, 39–50 (2003).
6. **Schwartz, M. A. and Ginsberg, M. H.:** Networks and crosstalk: integrin signalling spreads. Nat. Cell Biol., **4**, 65–68 (2002).
7. **Curtis, A. and Wilkinson, C.:** Topographical control of cells. Biomaterials, **18**, 1573–1583 (1997).
8. **Frey, M. T., Tsai, I. Y., Russell, T. P., Hanks, S. K., and Wang, Y.-I.:** Cellular response to substrate topography: role of myosin II and focal adhesion kinase. Biophys. J., **90**, 3774–3782 (2006).
9. **Mustafa, K., Odén, A., Wennerberg, A., Hultenby, K., and Arvidson, K.:** The influence of surface topography of ceramic abutments on the attachment and proliferation of human oral fibrablasts. Biomaterials, **26**, 373–381 (2005).
10. **Ponsonnet, L., Comte, V., Othmane, A., Lagneau, C., Charbonnier, M., Lissac, M., and Jaffrezic, N.:** Effect of surface topography and chemistry on adhesion, orientation and growth of fibroblasts on nickel-titanium substrates. Mater. Sci. Eng. C, **21**, 157–165 (2002).
11. **Hatano, K., Inoue, H., Kojo, T., Matsunaga, T., Tsujisawa, T., Uchiyama, C., and Uchida, Y.:** Effect of surface roughness on proliferation and alkaline phosphatase expression of rat calvarial cells cultured on polystyrene. Bone, **25**, 439–445 (1999).
12. **Fan, Y. W., Cui, F. Z., Hou, S. P., Xu, Q. Y., Chen, L. N., and Lee, I.-S.:** Culture of neural cells on silicon wafers with nano-scale surface topography. J. Neurosci. Methods, **120**, 17–23 (2002).
13. **Dalby, M. J.:** Topographically induced direct cell mechanotransduction. Med. Eng. Phys., **27**, 730–742 (2005).
14. **Curran, J. M., Chen, R., and Hunt, J. A.:** The guidance of human mesenchymal stem cell differentiation *in vitro* by controlled modifications to the cell substrate. Biomaterials, **27**, 4783–4793 (2006).
15. **Yim, E. K. and Leong, K. W.:** Significance of synthetic nanostructures in dictating cellular response. Nanomedicine, **1**, 10–21 (2005).
16. **Diehl, K. A., Foley, J. D., Nealey, P. F., and Murphy, C. J.:** Nanoscale topography modulates corneal epithelial cell mi-

gration. J. Biomed. Mater. Res., **75A**, 603–611 (2005).
17. **Loesberg, W. A., Walboomers, X. F., van Loon, J. J. W. A., and Jansen, S. A.:** The effect of combined hypergravity and microgrooved surface topography on the behaviour of fibroblast. Cell Motil. Cytoskeleton, **63**, 384–394 (2006).
18. **Lee, C. C., Mackay, J. A., Fréchet, J. M. J., and Szoka, F. C.:** Designing dendrimers for biological applications. Nat. Biotechnol., **23**, 1517–1526 (2005).
19. **Tomalia, D. A., Huang, B., Swanson, D. R., Brothers, H. M., and Klimash, J. W.:** Structure control within poly (amidoamine) dendrimers: size, shape and region-chemical mimicry of globular proteins. Tetrahedron, **59**, 3799–3813 (2003).
20. **Bielinska, A., Kukowska-Latallo, J. F., Johnson, J., Tomalia, D. A., and Baker, J. R., Jr.:** Regulation of *in vitro* gene expression using antisense oligonucleotides or antisense expression plasmids transfected using starburst PAMAM dendrimers. Nucleic Acids Res., **24**, 2176–2182 (1996).
21. **Lai, J. C., Yuan, C., and Thomas, J. L.:** Single-cell measurements of polyamidoamine dendrimer binding. Ann. Biomed. Eng., **30**, 409–416 (2002).
22. **Kawase, M., Kurikawa, N., Higashiyama, S., Miura, N., Shiomi, T., Ozawa, C., Mizoguchi, T., and Yagi, K.:** Immobilization of ligand-modified polyamidoamine dendrimer for cultivation of hepatoma cells. Artif. Org., **24**, 18–22 (2000).
23. **Kawase, M., Kurikawa, N., Higashiyama, S., Miura, N., Shiomi, T., Ozawa, C., Mizoguchi, T., and Yagi, K.:** Effectiveness of polyamidoamine dendrimers modified with tripeptide growth factor, glycyl-L-histidyl-L-lysine, for enhancement of function of hepatoma cells. J. Biosci. Bioeng., **88**, 433–437 (1999).
24. **Higashiyama, S., Noda, M., Kawase, M., and Yagi, K.:** Mixed-ligand modification of polyamidoamine dendrimers to develop an effective scaffold for maintenance of hepatocyte spheroids. J. Biomed. Mater. Res., **64A**, 475–482 (2003).
25. **Hata, N., Kim, M.-H., Isoda, K., Kino-oka, M., Kawase, M., Yagi, K., and Taya, M.:** Dendrimer-immobilized culture surface as a tool to evaluate formation of cellular cytoskeleton of anchorage-dependent cells. J. Biosci. Bioeng., **97**, 222–238 (2004).
26. **Gilbert, M., Giachelli, C. M., and Styton, P. S.:** Biomimetic peptides that engage specific integrin-dependent signaling pathways and bind to calcium phosphate surfaces. J. Biomed. Mater. Res., **67A**, 69–77 (2003).
27. **García, A. J.:** Get a grip: integrins in cell-biomaterial interactions. Biomaterials, **26**, 7525–7529 (2005).
28. **Hersel, U., Dahmen, C., and Kessler, H.:** RGD modified polymers: biomaterials for stimulated cell adhesion and beyond. Biomaterials, **24**, 4385–4415 (2003).
29. **García, A. J. and Reyes, C. D.:** Engineering integrin-specific surfaces with a triple-helical collagen-mimetic peptide. J. Biomed. Mater. Res., **65A**, 511–523 (2003).
30. **Lieb, E., Hacker, M., Tessmar, J., Kunz-Schughart, L. A., Fiedler, J., Dahmen, C., Hersel, U., Kessler, H., Schulz, M. B., and Göpferich, A.:** Mediating specific cell adhesion to low-adhesive diblock copolymers by instant modification with cyclic RGD peptides. Biomaterilas, **26**, 2333–2341 (2005).

Incorporation of Capillary-Like Structures into Dermal Cell Sheets Constructed by Magnetic Force-Based Tissue Engineering

Kosuke INO[1,2], Akira ITO[3], Hirohito KUMAZAWA[1], Hideaki KAGAMI[4], Minoru UEDA[5] and Hiroyuki HONDA[1]

[1]*Department of Biotechnology, School of Engineering, Nagoya University, Furo-cho, Chikusa-ku, Nagoya-shi, Aichi 464-8603, Japan*

[2]*Reseach Fellow of the Japan Society for the Promotion of Science (JSPS Research Fellow), Japan*

[3]*Department of Chemical Engineering, Faculty of Engineering, Kyushu University, 744, Motooka, Nishi-ku, Fukuoka-shi, Fukuoka 819-0395, Japan*

[4]*Department of Tissue Engineering, School of Medicine, Nagoya University, 65, Turumai-cho, Showa-ku, Nagoya-shi, Aichi 466-8550, Japan*

[5]*Department of Oral and Maxillofacial Surgery, School of Medicine, Nagoya University, 65, Turumai-cho, Showa-ku,, Nagoya-shi, Aichi 466-8550, Japan*

Keywords: Magnetite Nanoparticle, Liposome, Angiogenesis, Co-culture, Dermis

One of the major challenges in tissue engineering remains the construction of vascularized 3D transplants *in vitro*. We recently proposed novel technologies, termed "magnetic force-based tissue engineering" (Mag-TE), to establish three-dimensional (3D) tissues without using scaffolds. Magnetite cationic liposomes (MCLs), which contain 10-nm magnetite nanoparticles in order to improve accumulation of magnetite nanoparticles in target cells, were used to magnetically label normal human dermal fibroblasts (NHDFs). Magnetically labeled NHDFs were seeded onto ultralow-attachment plates. When a magnet was placed under the plate, cells accumulate on the bottom of the well. After a 24-h-incubation period, the cells form a sheet-like structure, which contains the major dermal extracellular matrix (ECM) components (fibronectin and type I collagen) within the NHDF sheet. Human umbilical vein endothelial cells (HUVECs) were co-cultured with NHDF sheets by two methods: HUVECs and NHDFs were mixed and then allowed to form cell sheets by Mag-TE; or NHDF sheets were constructed by Mag-TE and HUVECs were subsequently seeded onto NHDF sheets. These methods gave tube-like formation of HAECs, resembling early capillaries, within or on the surface NHDF sheets after short-term 3D co-culture, thus suggesting that Mag-TE may be useful for constructing 3D-tissue involving capillaries.

Introduction

Tissue engineering is a promising technology for repairing defective tissues *in vivo*. Tissue engineering can be used to restore, or enhance the function of defective tissues. There are three main approaches to tissue engineering: (1) to use isolated cells and/or cell substitutes as cellular replacement parts, (2) to use acellular biomaterials capable of inducing tissue regeneration, and (3) to use a combination of cells and materials. Tissue engineering is generally based on the seeding of cells onto three-dimensional (3D) porous biodegradable scaffolds for constructing 3D tissue structures (Langer and Vacanti, 1993). These scaffolds allow the cells to form a 3D tissue structure via cell adhesion, proliferation and deposition of extracellular matrix (ECM). Problems with this approach include insufficient cell migration into the scaffolds, which may cause a crucial prolongation of the culture period due to a shortage of initially seeded cells, and inflammatory reactions to byproducts of scaffold biodegradation. To overcome these disadvantages, novel alternative approaches to creating 3D tissue constructs are needed.

Magnetite particles of nanometer to submicron size have been used in an increasing number of biological and medical applications (Shinkai and Ito, 2004). The unique feature of the magnetite particle is its reaction to magnetic force. Magnetite particles have been used for cell sorting, as high magnetic flux density attracts magnetically labeled cells (Miltenyi *et al.*, 1990; Radbruch *et al.*, 1994; Moore *et al.*, 1998; Lewin

Received on May 29, 2006. Correspondence concerning this article should be addressed to H. Honda (E-mail address: honda@nubio.nagoya-u.ac.jp).

et al., 2000). We previously developed magnetite cationic liposomes (MCLs), which contain 10-nm magnetite nanoparticles, in order to improve accumulation of magnetite nanoparticles in target cells, due to electrostatic interaction between MCLs and the cell membrane (Shinkai *et al.*, 1996). In addition, we recently developed a novel tissue engineering technique using MCLs, based on the fact that cells labeled with MCLs can be manipulated using magnetic force (Ito *et al.*, 2004a, 2004c, 2005a, 2005c; Shimizu *et al.*, 2005). With this technique, we used a magnet to accumulate magnetically labeled keratinocytes onto a culture surface, and sheet-like multi-layered 3D constructs were successfully created without using any artificial polymer scaffolds (Ito *et al.*, 2004a). Thus, we developed a novel methodology for tissue engineering using magnetite nanoparticles and magnetic force, which we designated "magnetic force-based tissue engineering (Mag-TE)".

Neovascularization is a critical obstacle yet to be overcome in the engineering of tissue constructs larger than a few cubic millimeters. Thick and large 3D tissue constructs require vascularization *in vitro*, which is able to maintain cell viability during tissue growth, induce structural organization and promote vascularization after implantation. Thus, it is necessary to develop a novel methodology to construct 3D tissues involving capillaries. In the present study, we investigated whether angiogenesis could be induced in 3D tissues constructed by Mag-TE. Angiogenesis is a complex process involving numerous growth factors, extracellular matrix (ECM) (Sengar, 1996; Sephel *et al.*, 1996), enzymes (Lorimier *et al.*, 1996; Weckoth *et al.*, 1996) and co-existing cell types *in vivo* (Schaffer and Nanney, 1996). In the present study, we investigated whether ECM components, such as type I collagen and fibronectin, which have the capacity to induce angiogenesis, are deposited in normal human dermal fibroblast (NHDF) sheets constructed by Mag-TE, and whether human umbilical vein endothelial cells (HUVECs) form capillaries during 3D co-culture with NHDF sheets. Furthermore, we periodically observed these capillaries in details, and show the processes of capillary formation were similar to that during early angiogenesis *in vivo*.

1. Materials and Methods

1.1 Cells and culture

HUVECs, NHDFs and normal human epidermal keratinocytes (NHEKs) were provided as frozen cells after primary culture by the supplier (Kurabo Industries Ltd.), and were cultured in commercially available growth media (HuMedia-EG2 for HUVECs, Medium106S for NHDFs, and HuMedia-KG2 for NHEKs; Kurabo) at 37°C in a humidified atmosphere of CO_2 and 95% air.

1.2 Preparation of magnetite cationic liposomes

Magnetite (Fe_3O_4; average particle size, 10 nm; Toda Kogyo) was used as the core of the MCLs. MCLs were prepared using colloidal magnetite and a lipid mixture of *N*-(α-trimethylammonioacetyl)-didodecyl-D-glutamate chloride (TMAG, a cationic lipid; Sogo Pharmaceutical Co.), dilauroylphosphatidyl-choline (DLPC; Sigma Chemical Co.), and dioleoylphosphatidyl-ethanolamine (DOPE; Avanti Polar Lipids Inc.) in a molar ratio of 1:2:2, as described previously (Shinkai *et al.*, 1996). Average MCL particle size was 150 nm, and was measured using a dynamic light scattering spectrophotometer (FRAR 1000, Otsuka Electronics Co., Ltd.).

1.3 MCL uptake by cells

Uptake of MCLs by HUVECs or NHDFs was examined as described previously (Shinkai *et al.*, 1996). Briefly, HUVECs or NHDFs were seeded into a 60-mm cell culture dish (Asahi Techno Glass Corp.). After a 24-h incubation period, the medium was replaced with MCL-containing medium (net magnetite concentration, 100 pg/cell) and cells were incubated further. To assay magnetite uptake, cells were sampled periodically, and iron concentration and the number of viable cells were measured using the potassium thiocyanate method (Owen and Sykes, 1984) and the dye-exclusion method with trypan blue, respectively.

1.4 Construction of cell sheets using MCLs and magnetic force (Mag-TE)

NHDFs were cultured until subconfluent, and medium were replaced with flesh medium containing MCLs (net magnetite concentration, 100 pg/cell). After 24 h of culture with MCLs, the medium were removed, and the cells were rinsed with phosphate-buffered saline (PBS) to remove the medium completely. Then, the cells were harvested by trypsin treatment. Magnetically labeled NHDFs (2×10^6 cells) were seeded into a 24-well ultralow-attachment plate (culture area, 200 mm^2, Corning Inc.), the surface of which is comprised of a covalently bound hydrogel layer that was hydrophilic and neutrally charged. A cylindrical neodymium magnet (diameter, 30 mm; height, 15 mm; magnetic induction, 0.40 T) was then placed at the reverse side of the ultralow-attachment plate in order to provide magnetic force vertical to the plate, and cells were cultured for 1 d. We designated this procedure "Mag-TE".

1.5 Construction of NHDF sheets by mixing HUVECs with NHDFs

In order to label cells magnetically, MCLs (net magnetite concentration, 100 pg/cell) were added to both NHDFs and HUVECs and cells were incubated for 24 h. Cells were harvested, and HUVECs (6×10^4 cells) were mixed with NHDFs (1.8×10^6 cells). The mixture was seeded onto ultra-low-attachment plates. A cylindrical neodymium magnet was then placed at the reverse side of the plate in order to provide magnetic